

Syntheses, structures, and magnetic properties of the europium(II) selenido pnictogenates(III), EuPnSe_3 ($Pn = \text{Sb, Bi}$)

Geng Bang Jin^a, Shane J. Crerar^b, Arthur Mar^b, Thomas E. Albrecht-Schmitt^{a,*}

^aDepartment of Chemistry and Biochemistry, Auburn University, Auburn, AL 36849, USA

^bDepartment of Chemistry, University of Alberta, Edmonton, Alberta, T6G 2G2, Canada

Received 14 September 2005; received in revised form 30 January 2006; accepted 12 February 2006

Available online 20 March 2006

Abstract

EuPnSe_3 ($Pn = \text{Sb, Bi}$) have been synthesized through the reaction of Eu with Pn_2Se_3 ($Pn = \text{Sb, Bi}$) and Se at 850–900 °C. These compounds are isotypic with SrPnSe_3 ($Pn = \text{Sb, Bi}$) and consist of square pyramidal PnSe_5 units and distorted PnSe_6 octahedra that form hollow columns that extend along the c -axis. These columns are separated by Eu^{2+} cations that occur as nine-coordinate tricapped trigonal prisms. There are also additional V-shaped triselenide Se_3^{2-} anions between the columns that bind the Eu^{2+} cations. The $\text{Se}\cdots\text{Se}$ contacts (in EuSbSe_3) in these units are 2.4584(11) and 2.4359(11) Å, which are consistent with Se–Se single bonds. The overall structure is chiral. Bond-valence sum calculations indicate that these compounds contain Eu^{2+} . Magnetic susceptibility measurements provide values of 7.66 μ_B/Eu for EuSbSe_3 and 7.64 μ_B/Eu for EuBiSe_3 , which are close to the expected free-ion moment for Eu^{2+} . These compounds follow essentially Curie behavior from 300 to 5 K, and undergo an apparently antiferromagnetic transition below 5 K. Crystallographic data: EuSbSe_3 , orthorhombic, space group $P2_12_12_1$, $a = 32.936(2)$ Å, $b = 15.406(1)$ Å, $c = 4.2622(3)$ Å, $V = 2162.7(2)$ Å³, $Z = 16$, $R(F) = 2.63\%$ for 183 parameters and 5095 reflections with $I > 2\sigma(I)$; EuBiSe_3 , orthorhombic, space group $P2_12_12_1$, $a = 33.307(2)$ Å, $b = 15.5804(9)$ Å, $c = 4.2274(2)$ Å, $V = 2193.7(2)$ Å³, $Z = 16$, $R(F) = 2.68\%$ for 183 parameters and 4895 reflections with $I > 2\sigma(I)$.

© 2006 Elsevier Inc. All rights reserved.

Keywords: Europium antimony selenide; Europium bismuth selenide; Divalent europium; Crystal structure

1. Introduction

Ternary europium pnictogen chalcogenide compounds form a rich group that is currently represented by EuPn_2Q_4 ($Pn = \text{Sb, Bi}$; $Q = \text{S, Se, Te}$) [1,2], EuSb_4S_7 [2], $\text{Eu}_3\text{Sb}_4\text{S}_9$ [3], $\text{Eu}_{1.1}\text{Bi}_2\text{S}_4$ [4], Eu_2BiS_4 [5], EuPn_4Q_7 ($Pn = \text{Sb, Bi}$; $Q = \text{S, Se}$) [6], $\text{Eu}_3\text{Pn}_4\text{Q}_9$ ($Pn = \text{Sb, Bi}$; $Q = \text{S, Se, Te}$) [6], $\text{Eu}_6\text{Sb}_6\text{S}_{17}$ [7], and the metal-rich phase $\text{Eu}_4\text{Bi}_2\text{Te}$ [8]. The structures and properties of many of these compounds have been reviewed by Carré and co-workers [9]. In addition to adopting novel structure types, these compounds possess interesting electronic properties that are often associated with the divalent or mixed-valent character of the Eu ions. Many of the aforementioned compounds contain Eu(II), which can be rationalized by the stability of the half-filled $4f^7$ shell. Eu_2BiS_4 contains both Eu(II) and Eu(III) in different crystallographic

sites [5]. The transport and magnetic properties of many of these compounds have been measured. In this regard, one of the more interesting phases is Eu_2BiS_4 , which displays semi-metallic behavior ascribed to the mobility of electrons inside hexagonal channels within the structure [9].

While europium pnictogen sulfides have good representation, less is known about selenides and tellurides. In an effort to better understand this system we have prepared the new phases EuPnSe_3 ($Pn = \text{Sb, Bi}$), which proved to be isotypic with SrPnSe_3 ($Pn = \text{Sb, Bi}$) [10,11], determined their crystal structures, and measured their magnetic properties, which are reported herein.

2. Experimental

2.1. Syntheses

Eu (99.9%, Alfa-Aesar), Sb (99.5%, Alfa-Aesar), Bi (99.5%, Alfa-Aesar), and Se (99.5%, Alfa-Aesar) were used as received.

*Corresponding author. Fax: +1 334 844 6959.

E-mail address: albreth@auburn.edu (T.E. Albrecht-Schmitt).

Sb₂Se₃ and Bi₂Se₃ were prepared from the direct reaction of the elements in sealed fused-silica ampoules at 850 °C.

2.2. EuPnSe₃

EuSbSe₃: Eu (0.0595 g, 0.392 mmol), Sb₂Se₃ (0.0941 g, 0.196 mmol), and Se (0.0464 g, 0.588 mmol) or for *EuBiSe₃*: Eu (0.0508 g, 0.334 mmol), Bi₂Se₃ (0.1095 g, 0.167 mmol), and Se (0.0396 g, 0.501 mmol) were loaded into fused-silica ampoules that were then sealed under vacuum. The following heating profiles were used: *EuSbSe₃*—2 °C/min from room temperature to 500 °C where it was held for 1 h, 0.5 °C/min to 850 °C where it was held for 6 d, 0.04 °C/min to 400 °C where it was held 2 d, and 0.5 °C/min to 24 °C; *EuBiSe₃*: 2 °C/min to 600 °C where it was held for 1 h, 0.5 °C/min to 900 °C where it was held for 4 d, 0.03 °C/min to 500 °C where it was held for 1 d, and 0.5 °C/min to 24 °C. In both cases the products consisted of thin black needles up to 2 mm in length. PXRD measurements confirmed phase purity by comparison with powder patterns calculated from the single crystal X-ray structures. Semi-quantitative SEM/EDX analyses were performed using a JEOL 840/Link Isis instrument. Eu, Sb, Bi, and Se percentages were calibrated against standards. The Eu:Pn(Sb, Bi):Se ratio determined from EDX analyses were approximately 1:1:3.

2.3. Crystallographic studies

Single crystals of *EuSbSe₃* and *EuBiSe₃* were mounted on glass fibers and aligned on a Bruker SMART APEX

CCD X-ray diffractometer and cooled to 193 K using an Oxford Cryostat. Intensity measurements were performed using graphite monochromated MoK α radiation from a sealed tube and monocapillary collimator. SMART (v 5.624) was used for preliminary determination of the cell constants and data collection control. The intensities of reflections of a sphere were collected by a combination of 3 sets of exposures (frames). Each set had a different ϕ angle

Table 2
Atomic coordinates and equivalent isotropic displacement parameters for *EuSbSe₃*

Atom (site)	x	y	z	U_{eq} (Å ²) ^a
Eu(1)	0.576979(10)	0.57063(2)	0.49241(10)	0.01218(8)
Eu(2)	0.296366(10)	0.13685(2)	0.02213(11)	0.01185(8)
Eu(3)	0.328241(11)	0.78806(2)	0.55498(9)	0.01190(8)
Eu(4)	0.540637(11)	0.22202(3)	0.98005(11)	0.01640(9)
Sb(1)	0.863350(19)	0.94069(4)	0.97073(16)	0.02636(13)
Sb(2)	0.73758(2)	0.87685(4)	0.95831(17)	0.03376(17)
Sb(3)	0.522404(14)	0.96358(3)	0.48936(14)	0.01751(11)
Sb(4)	0.612807(16)	0.80824(3)	0.95840(15)	0.01861(12)
Se(1)	0.58106(2)	0.02102(6)	0.9515(3)	0.0280(2)
Se(2)	0.68091(2)	0.84877(5)	0.4793(3)	0.0260(2)
Se(3)	0.80227(2)	0.91220(6)	0.4644(4)	0.0344(3)
Se(4)	0.28659(2)	0.98044(4)	0.5007(2)	0.01259(14)
Se(5)	0.63578(2)	0.65000(4)	0.9772(2)	0.01173(14)
Se(6)	0.26013(2)	0.78192(5)	0.03648(19)	0.01229(15)
Se(7)	0.43833(2)	0.27777(5)	0.0203(2)	0.01714(16)
Se(8)	0.38870(2)	0.71799(5)	0.0379(2)	0.01347(15)
Se(9)	0.39990(2)	0.92243(5)	0.5091(2)	0.01271(14)
Se(10)	0.51079(2)	0.61894(5)	0.0084(2)	0.01391(14)
Se(11)	0.47580(2)	0.89768(5)	0.9407(2)	0.0219(2)
Se(12)	0.34292(2)	0.94859(5)	0.14871(18)	0.01230(16)

^a U_{eq} is defined as one-third of the trace of the orthogonalized U_{ij} tensor.

Table 1
Crystallographic data for *EuSbSe₃* and *EuBiSe₃*

Formula	<i>EuSbSe₃</i>	<i>EuBiSe₃</i>
Formula mass	510.59	597.82
Color and habit	Black needle	Black needle
Crystal system	Orthorhombic	Orthorhombic
Space group	<i>P</i> 2 ₁ 2 ₁ 2 ₁ (No. 19)	<i>P</i> 2 ₁ 2 ₁ 2 ₁ (No. 19)
<i>a</i> (Å)	32.936(2)	33.307(2)
<i>b</i> (Å)	15.406(1)	15.5804(9)
<i>c</i> (Å)	4.2622(3)	4.2274(2)
<i>V</i> (Å ³)	2162.7(2)	2193.7(2)
<i>Z</i>	16	16
<i>T</i> (K)	193	193
λ (Å)	0.71073	0.71073
Maximum 2 θ (deg.)	56.74	56.58
<i>R</i> (int)	0.0430	0.0494
Reflections (total)	21782	22502
Reflections (ind.)	5410	5470
Parameter	182	183
Weighting scheme	0.0298	0.0190
Res. electron den. (min,max)	−3.029, 2.044	−1.721, 2.856
ρ_{calcd} (g cm ^{−3})	6.273	7.240
μ (Mo K α) (cm ^{−1})	365.10	631.10
<i>R</i> (<i>F</i>) for $F_o^2 > 2\sigma(F_o^2)$ ^a	0.0263	0.0268
<i>R</i> _w (F_o^2) ^b	0.0612	0.0538

$$^a R(F) = \frac{\sum ||F_o| - |F_c||}{\sum |F_o|}$$

$$^b R_w(F_o^2) = \frac{[\sum [w(F_o^2 - F_c^2)]^2]}{\sum wF_o^4}]^{1/2}$$

Table 3
Atomic coordinates and equivalent isotropic displacement parameters for *EuBiSe₃*

Atom (site)	x	y	z	U_{eq} (Å ²) ^a
Eu(1)	0.423100(13)	0.43651(3)	0.50871(15)	0.01152(10)
Eu(2)	0.703237(13)	0.86713(3)	0.97886(15)	0.01120(10)
Eu(3)	0.673097(14)	0.21559(3)	0.44798(12)	0.01090(11)
Eu(4)	0.457513(14)	0.78660(3)	0.01679(16)	0.01635(11)
Bi(1)	0.139593(10)	0.05145(2)	0.01155(12)	0.01252(8)
Bi(2)	0.265127(10)	0.12156(2)	0.01405(12)	0.01250(8)
Bi(3)	0.478387(10)	0.04741(2)	0.51028(11)	0.01252(8)
Bi(4)	0.389701(10)	0.19634(2)	0.01923(12)	0.01215(8)
Se(1)	0.41803(3)	0.98808(6)	0.0436(3)	0.0124(2)
Se(2)	0.32141(3)	0.15262(6)	0.5316(3)	0.0127(2)
Se(3)	0.20035(3)	0.08477(6)	0.5422(3)	0.0118(2)
Se(4)	0.71366(2)	0.02172(6)	0.5002(3)	0.01103(18)
Se(5)	0.36444(3)	0.35747(6)	0.0229(3)	0.01081(19)
Se(6)	0.74097(3)	0.21586(6)	0.9655(3)	0.0109(2)
Se(7)	0.55806(3)	0.73215(6)	0.9767(3)	0.01188(19)
Se(8)	0.61263(3)	0.28598(6)	0.9668(3)	0.0116(2)
Se(9)	0.60217(3)	0.08292(6)	0.4901(3)	0.01185(19)
Se(10)	0.48925(3)	0.38643(6)	−0.0049(3)	0.01159(18)
Se(11)	0.52751(3)	0.11325(6)	0.0509(2)	0.0119(2)
Se(12)	0.65795(3)	0.05528(7)	−0.1459(2)	0.0106(2)

^a U_{eq} is defined as one-third of the trace of the orthogonalized U_{ij} tensor.

for the crystal and each exposure covered a range of 0.3° in ω . A total of 1800 frames were collected with an exposure time per frame of 30 s for both compounds.

For EuSbSe_3 and EuBiSe_3 determination of integrated intensities and global refinement were performed with the Bruker SAINT (v 6.02) software package using a narrow-frame integration algorithm. A face-indexed numerical absorption correction was initially applied using XPREP [12]. These files were subsequently treated with a semi-empirical absorption correction by SADABS [13]. The program suite SHELXTL (v 6.12) was used for space group determination (XPREP), direct methods structure solution (XS), and least-squares refinement (XL) [12]. The final refinements included anisotropic displacement parameters for all atoms and secondary extinction. Some crystallographic details are given in Table 1. Atomic coordinates and equivalent isotropic displacement parameters for EuSbSe_3 and EuBiSe_3 can be found in Tables 2

and 3, respectively. Additional details can be found in the Supporting Information.

2.4. Magnetism

Magnetic susceptibility measurements were made between 2 and 300 K under zero-field-cooled conditions in an applied field of 0.5 T on a Quantum Design 9T-PPMS dc magnetometer/ac susceptometer. The susceptibility was corrected for contributions from the holder diamagnetism and the underlying sample diamagnetism.

3. Results and discussion

3.1. Structures of EuPnSe_3 ($Pn = \text{Sb, Bi}$)

EuSbSe_3 and EuBiSe_3 are isotypic with SrPnSe_3 ($Pn = \text{Sb, Bi}$) [10,11]. The structure of EuSbSe_3 will be

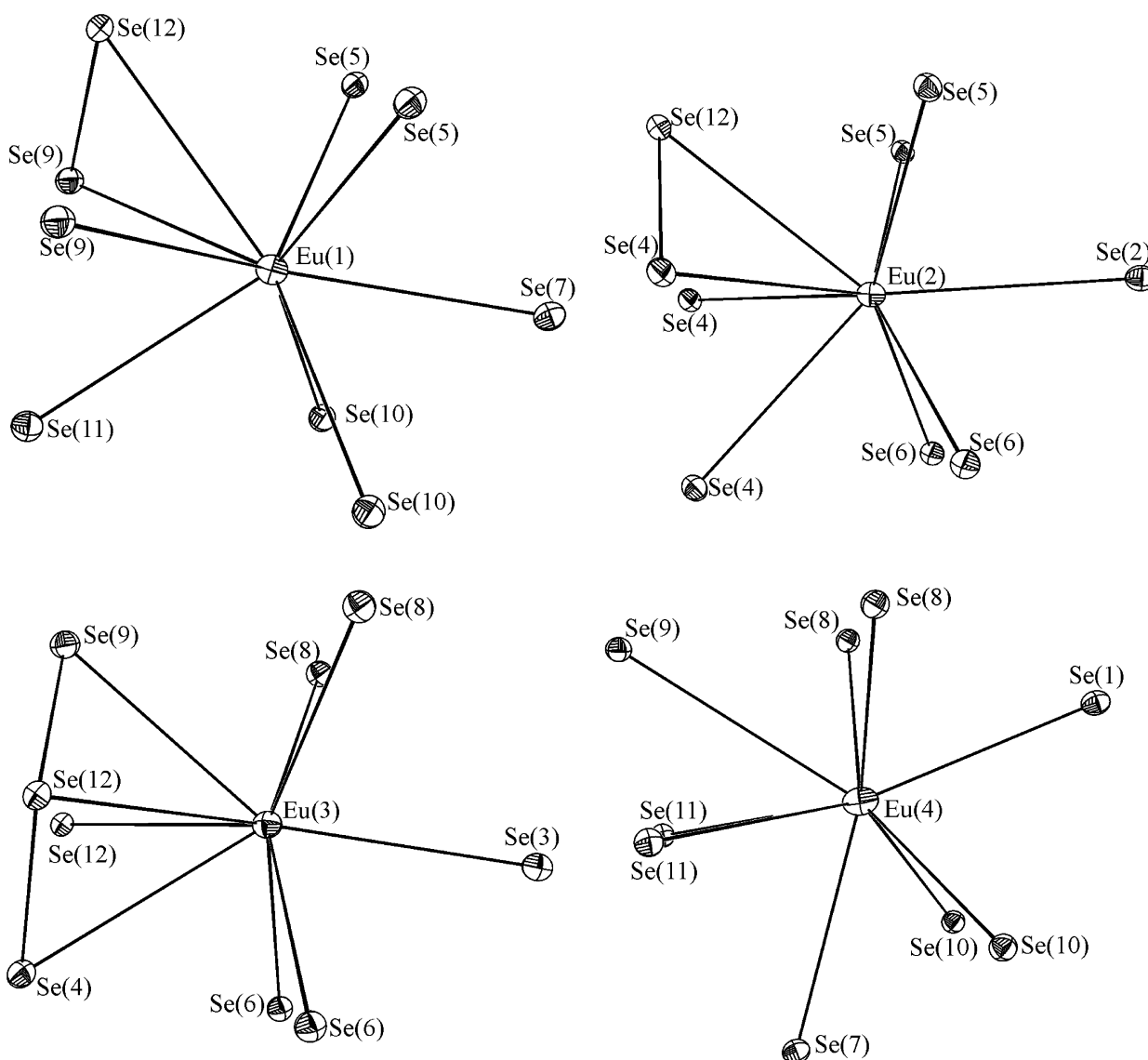


Fig. 1. Illustrations of the nine-coordinate tricapped trigonal prismatic environments around the Eu centers in EuSbSe_3 .

discussed with values for the Bi analog given parenthetically where important. There are four crystallographically unique Eu atoms in the structures of EuPnSe_3 . All four Eu sites are nine-coordinate and occur as tricapped trigonal prisms. Eu–Se bond distances range from 3.0846(9) to 3.2950(9) Å (3.0907(12) to 3.3240(11) Å), 3.0516(8) to 3.3496(9) Å (3.0587(11) to 3.4417(11) Å), 3.0419(8) to 3.5712(9) Å (3.0449(11) to 3.5773(12) Å), and 3.1052(9) to 3.7031(10) Å (3.1042(12) to 3.7447(10) Å) for Eu(1), Eu(2), Eu(3), and Eu(4), respectively. These polyhedra are shown in Fig. 1. Selected bond distances can be found in Tables 4 and 5. Bond-valence sum calculations provide values for the four Eu sites ranging from 1.60 to 2.27, implying Eu(II) character [14,15].

The coordination environments around the Sb centers are challenging to describe owing to the extreme variability in the Sb–Se bond lengths. For example, for Sb(3) there are three relatively short Sb–Se bonds of 2.6312(9), 2.6621(10),

2.8974(12) Å. If these are the sole contacts used then the geometry could be described as a distorted trigonal pyramid with a stereochemically active lone-pair of electrons. However, there are three longer contacts ranging from 2.9759(11)–3.1414(9) Å. It is probably best to describe this unit as a distorted octahedron. For Sb(1), Sb(2), and Sb(4) the sixth potential Sb...Se contact exceeds 3.4 Å, and these units are probably best described as square pyramids. The Sb and Se atoms form rectangular columns that extend down the *c*-axis as is shown in Fig. 2. These columns are formed from two opposing nets of square pyramidal SbSe_5 units that are linked by the SbSe_6 units (Fig. 3). The lone-pair of electrons on the Sb(III) centers appear to be contained within these columns. These rock-salt-like fragments are known from other ternary antimony and bismuth chalcogenide phases such as $\text{CsBi}_{3.67}\text{Se}_6$ [16], $\text{Sr}_4\text{Bi}_6\text{Se}_{13}$ [17], $A_{1+x}\text{Pb}_{4-2x}\text{Sb}_{7+x}\text{Se}_{15}$ ($A = \text{K}, \text{Rb}; 0 < x < 2$) [18].

Table 4
Selected bond distances (Å) for EuSbSe_3

Distances (Å)			
Eu(1)–Se(5)	3.0846(9)	Eu(4)–Se(8) #3	3.2083(9)
Eu(1)–Se(5) #1	3.1731(9)	Eu(4)–Se(9) #2	3.6567(8)
Eu(1)–Se(7) #4	3.2312(9)	Eu(4)–Se(10) #2	3.1183(9)
Eu(1)–Se(9) #2	3.2104(9)	Eu(4)–Se(10) #12	3.1850(9)
Eu(1)–Se(9) #3	3.2189(9)	Eu(4)–Se(11) #2	3.2911(10)
Eu(1)–Se(10) #1	3.0923(9)	Eu(4)–Se(11) #12	3.7031(10)
Eu(1)–Se(10)	3.1848(9)	Sb(1)–Se(1) #14	2.8108(12)
Eu(1)–Se(11) #2	3.1940(9)	Sb(1)–Se(1) #15	2.9323(13)
Eu(1)–Se(12) #2	3.2950(9)	Sb(1)–Se(3) #5	2.9438(14)
Eu(2)–Se(2) #3	3.3496(9)	Sb(1)–Se(3)	2.9829(13)
Eu(2)–Se(4) #8	3.1734(9)	Sb(1)–Se(8) #13	2.5834(10)
Eu(2)–Se(4) #6	3.2769(8)	Sb(2)–Se(2)	2.7999(12)
Eu(2)–Se(4) #9	3.2936(9)	Sb(2)–Se(2) #5	2.9329(14)
Eu(2)–Se(5) #3	3.0927(9)	Sb(2)–Se(3)	3.0442(15)
Eu(2)–Se(5) #2	3.0967(9)	Sb(2)–Se(3) #5	3.0804(13)
Eu(2)–Se(6) #6	3.0516(8)	Sb(2)–Se(6) #13	2.5562(9)
Eu(2)–Se(6) #7	3.1358(8)	Sb(3)–Se(1) #19	2.8974(12)
Eu(2)–Se(12) #9	3.3247(9)	Sb(3)–Se(1) #20	3.1257(11)
Eu(3)–Se(3) #10	3.2026(10)	Sb(3)–Se(7) #4	3.1414(9)
Eu(3)–Se(4)	3.2740(8)	Sb(3)–Se(10) #18	2.6312(9)
Eu(3)–Se(6) #5	3.0419(8)	Sb(3)–Se(11)	2.6621(10)
Eu(3)–Se(6)	3.1505(8)	Sb(3)–Se(11) #1	2.9759(11)
Eu(3)–Se(8) #5	3.0606(8)	Sb(4)–Se(2)	3.0969(12)
Eu(3)–Se(8)	3.1604(9)	Sb(4)–Se(2) #5	3.2172(11)
Eu(3)–Se(9)	3.1453(8)	Sb(4)–Se(5)	2.5537(9)
Eu(3)–Se(12) #1	3.0575(9)	Sb(4)–Se(7) #4	2.6870(10)
Eu(3)–Se(12)	3.5712(9)	Sb(4)–Se(7) #18	2.8272(11)
Eu(4)–Se(1)	3.3727(10)	Se(4)–Se(12) #5	2.4359(11)
Eu(4)–Se(7) #5	3.4814(9)	Se(12)–Se(9) #5	2.4584(11)
Eu(4)–Se(8) #2	3.1052(9)		

Symmetry transformations used to generate equivalent atoms:

#1 $x, y, z-1$; #2 $-x+1, y-1/2, -z+3/2$; #3 $-x+1, y-1/2, -z+1/2$; #4 $-x+1, y+1/2, -z+1/2$; #5 $x, y, z+1$; #6 $-x+1/2, -y+1, z-1/2$; #7 $-x+1/2, -y+1, z+1/2$; #8 $x, y-1, z$; #9 $x, y-1, z-1$; #10 $x-1/2, -y+3/2, -z+1$; #11 $x-1/2, -y+3/2, -z+2$; #12 $-x+1, y-1/2, -z+5/2$; #13 $x+1/2, -y+3/2, -z+1$; #14 $-x+3/2, -y+1, z+1/2$; #15 $-x+3/2, -y+1, z-1/2$; #16 $-x+3/2, -y+2, z+1/2$; #17 $x+1/2, -y+3/2, -z+2$; #18 $-x+1, y+1/2, -z+3/2$; #19 $x, y+1, z$; #20 $x, y+1, z-1$.

Table 5
Selected bond distances (Å) for EuBiSe_3

Distances (Å)			
Eu(1)–Se(5)	3.0907(12)	Eu(4)–Se(8) #3	3.1976(12)
Eu(1)–Se(5) #1	3.1714(12)	Eu(4)–Se(9)	3.7447(10)
Eu(1)–Se(7) #4	3.2457(11)	Eu(4)–Se(10) #2	3.1339(12)
Eu(1)–Se(9) #2	3.2187(13)	Eu(4)–Se(10) #11	3.2010(12)
Eu(1)–Se(9) #3	3.2251(13)	Eu(4)–Se(11) #2	3.2991(12)
Eu(1)–Se(10) #1	3.1130(12)	Eu(4)–Se(11) #11	3.6472(12)
Eu(1)–Se(10)	3.1901(12)	Bi(1)–Se(1) #13	2.8243(11)
Eu(1)–Se(11) #2	3.2177(11)	Bi(1)–Se(1) #14	3.0206(11)
Eu(1)–Se(12) #2	3.3240(11)	Bi(1)–Se(3) #5	2.8812(11)
Eu(2)–Se(2) #3	3.4417(11)	Bi(1)–Se(3)	3.0652(12)
Eu(2)–Se(4) #8	3.1647(12)	Bi(2)–Se(8) #12	2.6890(10)
Eu(2)–Se(4) #6	3.2663(10)	Bi(2)–Se(2) #5	2.8118(12)
Eu(2)–Se(4) #9	3.2833(13)	Bi(2)–Se(2)	2.9216(12)
Eu(2)–Se(5) #3	3.0889(12)	Bi(2)–Se(3) #5	2.9939(11)
Eu(2)–Se(5) #2	3.0988(12)	Bi(2)–Se(3)	3.1573(11)
Eu(2)–Se(6) #6	3.0587(11)	Bi(2)–Se(6) #12	2.6592(10)
Eu(2)–Se(6) #7	3.1360(12)	Bi(3)–Se(1) #16	2.9641(11)
Eu(2)–Se(12) #9	3.3387(12)	Bi(3)–Se(1) #17	3.1589(11)
Eu(3)–Se(3) #10	3.2405(11)	Bi(3)–Se(7) #4	3.1246(10)
Eu(3)–Se(4)	3.3164(10)	Bi(3)–Se(10) #15	2.7298(10)
Eu(3)–Se(6) #5	3.0449(11)	Bi(3)–Se(11)	2.7387(11)
Eu(3)–Se(6)	3.1459(11)	Bi(3)–Se(11) #1	2.9918(11)
Eu(3)–Se(8) #5	3.0657(12)	Bi(4)–Se(2) #5	3.1444(11)
Eu(3)–Se(8)	3.1731(12)	Bi(4)–Se(2)	3.2141(11)
Eu(3)–Se(9)	3.1440(10)	Bi(4)–Se(5)	2.6479(10)
Eu(3)–Se(12) #1	3.0725(12)	Bi(4)–Se(7) #15	2.7808(12)
Eu(3)–Se(12)	3.5773(12)	Bi(4)–Se(7) #4	2.8069(12)
Eu(4)–Se(1)	3.4053(11)	Se(4)–Se(12) #1	2.4400(14)
Eu(4)–Se(7) #5	3.4590(10)	Se(12)–Se(9) #1	2.4503(15)
Eu(4)–Se(8) #2	3.1042(12)		

Symmetry transformations used to generate equivalent atoms:

#1 $x, y, z+1$; #2 $-x+1, y+1/2, -z+1/2$; #3 $-x+1, y+1/2, -z+3/2$; #4 $-x+1, y-1/2, -z+3/2$; #5 $x, y, z-1$; #6 $-x+3/2, -y+1, z+1/2$; #7 $-x+3/2, -y+1, z-1/2$; #8 $x, y+1, z$; #9 $x, y+1, z+1$; #10 $x+1/2, -y+1/2, -z+1$; #11 $-x+1, y+1/2, -z-1/2$; #12 $x-1/2, -y+1/2, -z+1$; #13 $-x+1/2, -y+1, z-1/2$; #14 $-x+1/2, -y+1, z+1/2$; #15 $-x+1, y-1/2, -z+1/2$; #16 $x, y-1, z$; #17 $x, y-1, z+1$.

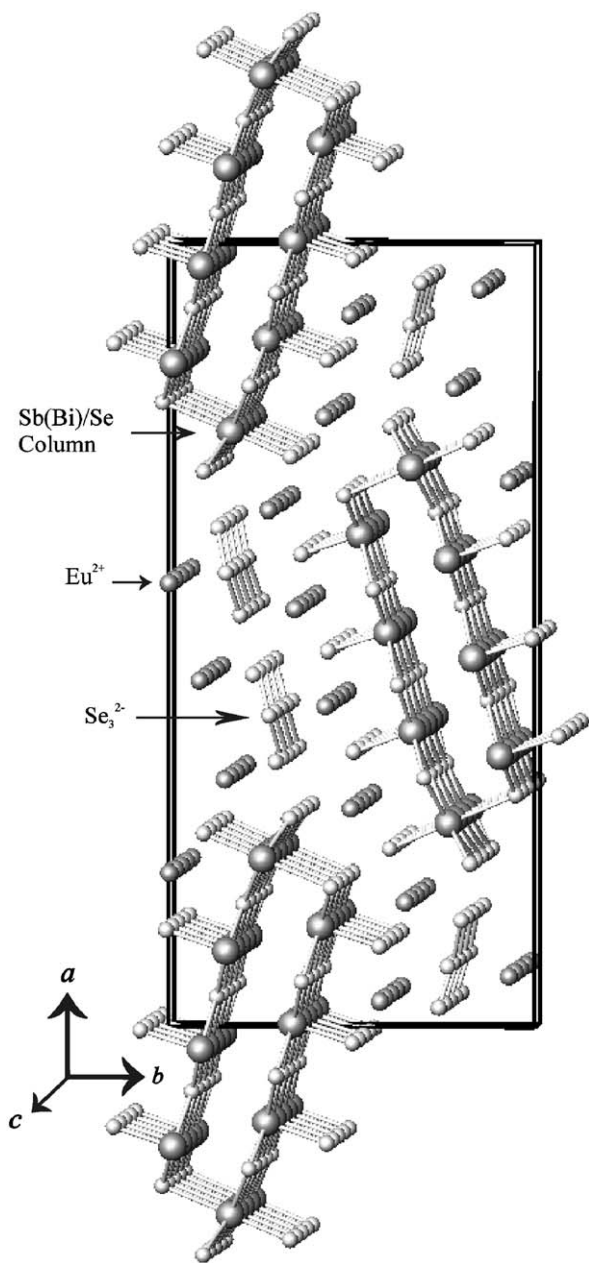


Fig. 2. A view of the one-dimensional rectangular columns formed from Pn ($Pn = Sb, Bi$) and Se in $EuPnSe_3$. These columns extend down the c -axis and are separated by Eu^{2+} cations and Se_3^{2-} anions.

In addition to the $Sb(Bi)/Se$ columns, there are also triselenide units. These V-shaped Se_3^{2-} anions are also aligned along the c -axis, and although they might be considered to be the most obvious source for the acentricity of $EuPnSe_3$ ($P2_12_12_1$ is chiral), groups of these units are aligned antiparallel with one another (see Fig. 2). The $Se \cdots Se$ contacts are 2.4584(11) and 2.4359(11) Å, and are typical of that expected for a single bond. For example, the $Se-Se$ bonds in the triselenide units in Sr_2SnSe_5 and Ba_2SnSe_5 range from 2.38 to 2.44 Å [19,20]. In $Eu_8(Sn_4Se_{14})(Se_3)_2$ the $Se-Se$ bonds in the triselenide units

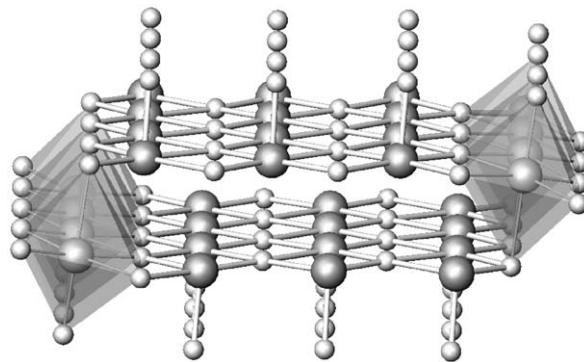


Fig. 3. A depiction of the Pn/Se columns in $EuPnSe_3$ ($Pn = Sb, Bi$) that are formed from two opposing nets of square pyramidal $PnSe_5$ units that are linked by $PnSe_6$ octahedra.

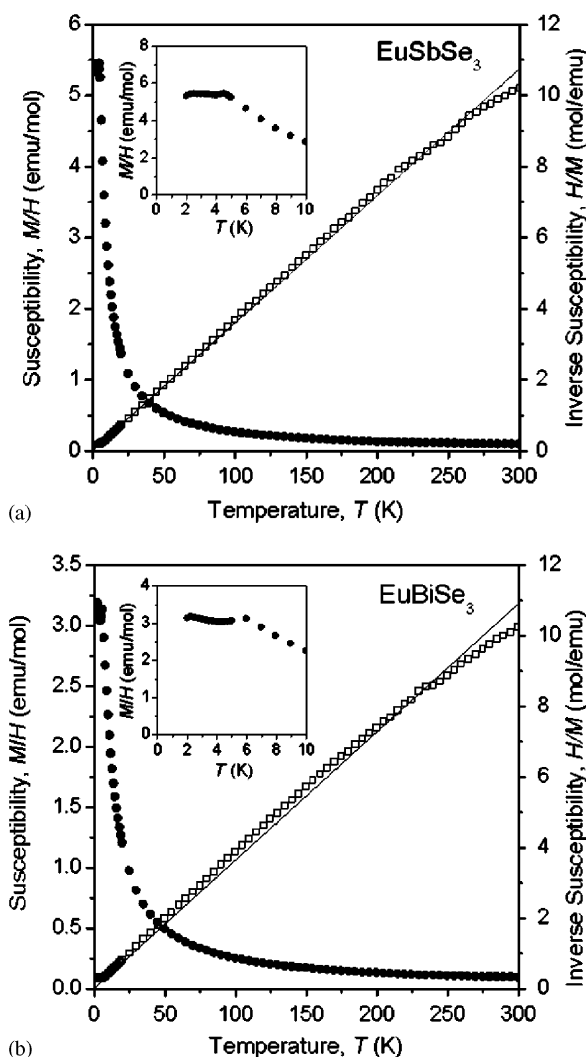


Fig. 4. Plots of dc magnetic susceptibility (\bullet) and its inverse (\diamond) for (a) $EuSbSe_3$ and (b) $EuBiSe_3$. The straight lines represent fits of the inverse susceptibility to the Curie–Weiss law. The insets show the low-temperature behaviour of the susceptibility.

are 2.398(2) and 2.416(2) [21]. $EuSbSe_3$ and $EuBiSe_3$ can then be formulated as $Eu^{2+} \times 4$ (for each crystallographically unique Eu center)/ $Pn^{3+} \times 4/Se^{2-} \times 9/Se_3^{2-}$.

3.2. Magnetic susceptibility

Plots of the zero-field-cooled molar magnetic susceptibility and its inverse for EuSbSe_3 and EuBiSe_3 from 2 to 300 K at an applied field of 5 kOe are shown in Fig. 4. Although the inverse susceptibility can be fit to the Curie–Weiss law, the Weiss constants are very small and close to zero (-0.5 to -1.0 K) for both compounds. The Curie constants are $27.9 \text{ emu K mol}^{-1}$ for EuSbSe_3 and $27.6 \text{ emu K mol}^{-1}$ for EuBiSe_3 , which correspond to an effective magnetic moment of $7.6 \mu_{\text{B}}$ per europium in both cases. As this value is only slightly smaller than the theoretical free-ion magnetic moment for Eu^{2+} ($7.9 \mu_{\text{B}}$), the presence of divalent europium is essentially confirmed. There is an apparent transition below 5 K in the susceptibility curves, but whether it can be clearly attributed to a long-range antiferromagnetic ordering remains to be further investigated.

4. Conclusions

In this work we have demonstrated that two new ternary europium pnictogen selenides, namely EuSbSe_3 and EuBiSe_3 , can be prepared via the reaction of Eu with Pn_2Se_3 ($\text{Pn} = \text{Sb, Bi}$) and Se. These compounds form as pure phases, and large single crystals exceeding 2 mm in length can be isolated. EuSbSe_3 and EuBiSe_3 possess complex structures containing one-dimensional antimony and bismuth selenide columns separated by Eu^{2+} cations and triselenide anions. Magnetic susceptibility measurements and bond-valence sum calculations are consistent with this compound containing Eu^{2+} .

Acknowledgments

This work was supported by the US Department of Energy under Grant DE-FG02-02ER45963.

Auxiliary Material: Further details of the crystal structure investigation may be obtained from the Fachinformationzentrum Karlsruhe, D-76344 Eggenstein-Leopoldshafen,

Germany (Fax: (+49)7247-808-666; Email: crysdata@fiz-karlsruhe.de) on quoting depository numbers CSD 415725 and 415724.

References

- [1] E.M. Godzhaev, P.G. Rustamov, M.S. Guseinov, O.M. Aliev, Russ. J. Phys. Chem. 52 (1978) 2424.
- [2] O.M. Aliev, P.G. Rustamov, G.G. Guseinov, M.S. Guseinov, Izvest. Akad. Nauk SSSR, Neorgan. Mater. 14 (1978) 1346.
- [3] P. Lemoine, D. Carré, M. Guittard, Acta Crystallogr. B 37 (1981) 1281.
- [4] P. Lemoine, D. Carré, M. Guittard, Acta Crystallogr. C 42 (1986) 259.
- [5] P. Lemoine, D. Carré, M. Guittard, Acta Crystallogr. B 38 (1982) 727.
- [6] O.M. Aliev, T.F. Maksudova, N.D. Samsonova, L.D. Finkel'shtein, P.G. Rustamov, Izvest. Akad. Nauk SSSR, Neorgan. Mater. 22 (1986) 29.
- [7] G. Jin, D.M. Wells, S.J. Crerar, T.C. Shehee, A. Mar, T.E. Albrecht-Schmitt, Acta Crystallogr. E 61 (2005) i116.
- [8] F. Hulliger, Mater. Res. Bull. 14 (1979) 259.
- [9] D. Carré, M. Guittard, S. Jaulmes, M. Julien-Pouzul, P. Lemoine, P. Laurelle, J. Flahaut, J. Less-Common Met. 110 (1985) 349.
- [10] R. Cook, H. Schäfer, Rev. Chim. Minér. 19 (1982) 19.
- [11] R. Cook, H. Schäfer, Stud. Inorg. Chem. 3 (1983) 757.
- [12] G.M. Sheldrick, SHELLXTL PC, Version 6.12, An Integrated System for Solving, Refining, and Displaying Crystal Structures from Diffraction Data, Siemens Analytical X-ray Instruments, Inc., Madison, WI, 2001.
- [13] G.M. Sheldrick, SADABS 2001, Program for absorption correction using SMART CCD based on the method of Blessing: R. H. Blessing, Acta Crystallogr. A 51 (1995) 33.
- [14] I.D. Brown, D. Altermatt, Acta Crystallogr. B 41 (1985) 244.
- [15] N.E. Brese, M. O'Keeffe, Acta Crystallogr. B 47 (1991) 192.
- [16] L. Iordanidis, P.W. Brazis, T. Kyratsi, J. Ireland, M. Lane, C.R. Kannewurf, W. Chen, J.S. Dyck, C. Uher, N.A. Ghelani, T. Hogan, M.G. Kanatzidis, Chem. Mater. 13 (2001) 622.
- [17] G. Cordier, H. Schäfer, C. Schwidetzky, Rev. Chim. Minér. 22 (1985) 631.
- [18] D.-Y. Chung, L. Iordanidis, K.-S. Choi, M.G. Kanatzidis, Bull. Kor. Chem. Soc. 19 (1998) 1281.
- [19] A. Assoud, N. Soheilnia, H. Kleinke, J. Solid State Chem. 178 (2005) 1087.
- [20] A. Assoud, N. Soheilnia, H. Kleinke, Chem. Mater. 16 (2004) 2215.
- [21] C.R. Evenson, P.K. Dorhout, Z. Anorg. Allg. Chem. 627 (2001) 2178.